13th ewtec 2019
Proceedings of the 13th European Wave and Tidal Energy Conference 1-6 Sept 2019, Naples, Italy

A stochastic method to account for the ambient turbulence in Lagrangian Vortex computations

Camille Choma Bex, Clément Carlier, Benoist Gaston,
Grégory Pinon, Grégory Germain, and Elie Rivoalen

***Abstract*—The ambient turbulence in the surrounding flow is of the utmost importance in the design of tidal turbine arrays, as it influences both the load and fatigue on each turbine and its wake. Various methods have been developed in order to replicate its effects in the context of Eulerian simulations, however none of these methods are easily transferable to a Lagrangian framework. This paper presents the adaptation of the Synthetic Eddy Method, originally formulated in order to generate turbulent inflows, to encompass the entire fluid domain in the background of a three-dimensional Vortex simulation code. The physical properties of the ensuing flows are analyzed, to better characterize the parameters of the model and ensure an adequate replication of experimental behaviors. These developments are carried out on the Vortex simulation code Dorothy developed at LOMC in collaboration with IFREMER for the simulation of tidal turbines.**

***Index Terms*—Numerical Simulation, SEM, Tidal Turbine, Turbulence, VPM, Wake.**

I. Introduction

THE ambient turbulence intensity in the upstream flow plays a determining role in the behavior of horizontal axis marine current turbines. Velocity fluctuations have an impact not only on the performances of an individual turbine, but also on the shape and length of its wake. This is of utmost importance in the design of marine turbine arrays, when considering the effect of a row of upstream turbines on the power output of any turbines positioned downstream.

Experimental studies in potential tidal sites have shown that turbulence intensity can range from approximately 3% to 20% [1]. Such non-negligible variations in inflow conditions must be taken into account when attempting to replicate numerically the true operating conditions of a tidal turbine.

The ID number of this paper is 1402 of the conference track THM: Tidal Hydrodynamic Modelling. Camille Choma Bex acknowledges the financial support of IFREMER for her Ph.D. grant. This work was also supported by the European ERDF and Normandy Regional Funding program NEPTUNE. The present work was performed on computing resources provided by CRIANN (Normandy, France).

C. Choma Bex and G. Germain are with Institut Français de Recherche pour l'Exploitation de la Mer (IFREMER), Centre Manche Mer du Nord, 150 quai Gambetta, BP 699, 62321 Boulogne-sur-Mer, France (email: camille.choma.bex@ifremer.fr).

C. Choma Bex and G. Pinon are with Laboratoire Ondes et Milieux Complexes (LOMC) - Normandie Univ, UNIHAVRE, CNRS, LOMC, 76600 Le Havre, France.

B. Gaston is with Centre Régional d'Informatique et Applications Numériques de Normandie (CRIANN), 745 Avenue de l'Université, 76800 Saint Etienne du Rouvray, France.

E. Rivoalen is with Laboratoire de Mécanique de Normandie (LMN) - Normandie Univ, INSA ROUEN, 76000 Rouen, France.

Various methods have been developed to emulate this ambient turbulence in the context of Eulerian simulations, through the use of boundary conditions. The Synthetic Eddy Method (SEM) proposed by Jarrin *et al.* [2] [3] was initially formulated within this context: its original purpose is to generate inflow conditions for the Eulerian simulation of turbulent flows using Large Eddy Simulation (LES).

However none of these methods can be applied as such to a Lagrangian framework. Thus, this paper deals with the adaptation and integration of the Synthetic Eddy Method proposed by Jarrin *et al.* to the context of Vortex simulation. First of all, an overview is given of the unsteady Lagrangian method. The adapted SEM is then presented and analyzed on a simple study case. Finally the combination of adapted SEM and Vortex methods is applied to the simulation of a simplified marine current turbine in varying turbulent conditions.

II. Numerical method

As a matter of nomenclature convention, bold signs will refer to vectors, regular letters will refer to continuous field (*e.g.* $\boldsymbol{u}$ for the continuous velocity field) and capital letters will refer to the corresponding discretised field (*e.g.* $\boldsymbol{U}_i$ for for the velocity of the i-th particle).

A. The Lagrangian Vortex method

An account of ambient turbulence has been integrated into the framework of a Vortex method computation [4]–[7]. This unsteady Lagrangian method is based on a discretisation of the flow into vorticity carrying particles. The governing equations for this unsteady and incompressible flow are the Navier-Stokes equations in their velocity/vorticity formulation.

The fluid domain is discretised into N particles, each particle i represented by its position $\boldsymbol{X}_i$ and its vortical weight $\boldsymbol{\Omega}_i$. The particles' transport over time is described by the following displacement equation, integrated using regular time stepping schemes:

$$\frac{\mathrm{d}\boldsymbol{X}_i}{\mathrm{d}t} = \boldsymbol{u}(\boldsymbol{X}_i) = \boldsymbol{U}_i. \tag{1}$$

This leads to a dicrestised formulation of the previously mentioned Navier-Stokes, dictating the evolution of the vorticity carried by each particle i:

$$\frac{\mathrm{d}\boldsymbol{\Omega}_i}{\mathrm{d}t} = \underbrace{(\boldsymbol{\Omega}_i \cdot \nabla)\,\boldsymbol{U}_i}_{\text{Stretching term:}\boldsymbol{\mathcal{S}}_i V_i} + \underbrace{\nu[\Delta\boldsymbol{\omega}]_{\boldsymbol{x}=\boldsymbol{X}_i} V_i}_{\text{Diffusion term:}\boldsymbol{\mathcal{L}}_i V_i} \tag{2}$$

The Lagrangian Vortex method is based on a Helmholtz decomposition of the velocity field:

$$\boldsymbol{U} = \underbrace{\nabla \wedge \boldsymbol{\psi}}_{\boldsymbol{U}^{\psi}} + \underbrace{\nabla\phi}_{\boldsymbol{U}^{\phi}} + \boldsymbol{U}^{\infty}, \tag{3}$$

where the components of the velocity can be summarized as the following:

- A rotational velocity component $\boldsymbol{U}^{\psi}$ accounting for particle-particle interaction, the core of any Lagrangian Vortex method.
- A potential velocity component $\boldsymbol{U}^{\phi}$, representing the influence of a solid body.
- A velocity component $\boldsymbol{U}^{\infty}$ representing the upstream velocity field at infinity, generally treated as a constant vector.

For a more comprehensive overview of the method and its implementation, see Pinon *et al.* [8]. The focus of this paper will be adapting the upstream velocity component $\boldsymbol{U}^{\infty}$ in order to account for ambient turbulence in the upstream flow, based on the Synthetic Method detailed in the next Section.

III. Ambient turbulence model in the Lagrangian framework

The aim of this study is to account for ambient turbulence in the fluid, with any given turbulence parameters and at any point in the study space. The Synthetic Eddy Method formulated by Jarrin *et al.* [2] [3] allows the generation of an input flow with any given turbulent intensity I_∞ and anisotropic ratio (σ_u:σ_v:σ_w). Within Jarrin's initial formulation, these turbulence conditions are only verified at the inlet of the fluid domain. Thus, this method must be adapted in order to encompass the entirety of a given study space.

The ambient turbulence intensity percentage I_∞ quantifies the velocity fluctuations in a three-dimensional flow $(u_\infty,\ v_\infty,\ w_\infty)$ as the following:

$$I_\infty = 100\sqrt{\frac{\frac{1}{3}\left[\sigma^2(u_\infty)+\sigma^2(v_\infty)+\sigma^2(w_\infty)\right]}{\bar{u}_\infty^2+\bar{v}_\infty^2+\bar{w}_\infty^2}} \tag{4}$$

B. General overview of the method

In the Synthetic Eddy Method proposed by Jarrin, ambient turbulence in the upstream flow is accounted for by modifying the upstream velocity component $\boldsymbol{u}^{\infty}$. This upstream velocity is rewritten via the Reynolds decomposition:

$$\boldsymbol{u}^{\infty}(\boldsymbol{x}) = \overline{\boldsymbol{u}^{\infty}} + \tilde{\boldsymbol{u}}(\boldsymbol{x}) \tag{5}$$

where $\overline{\boldsymbol{u}^{\infty}}$ is the mean velocity of the flow, and $\tilde{\boldsymbol{u}}$ a perturbation term representing the fluctuations due to ambient turbulence.

The perturbation term $\tilde{\boldsymbol{u}}$ is calculated as the influence of N "turbulent structures", also called "eddies", randomly positioned throughout a three-dimensional study space of volume $\tilde{V}$. Each "turbulent structure" k is characterized by its position $\boldsymbol{x}^k$ and its intensity $\boldsymbol{c}^k$, to be defined in the following paragraphs.

The perturbation induced by N turbulent structures is calculated as the sum of the influences of each structure k:

$$\tilde{\boldsymbol{u}}(\boldsymbol{x}) = \sum_{k=1}^{N} \tilde{\boldsymbol{u}}^k(\boldsymbol{x}), \tag{6}$$

with $\boldsymbol{x}$ a point of the fluid domain and $\tilde{\boldsymbol{u}}^k$ the perturbation velocity induced by a single turbulent structure k. This individual perturbation velocity is expressed as:

$$\tilde{\boldsymbol{u}}^k(\boldsymbol{x}) = \sqrt{\frac{\tilde{V}}{N}}\boldsymbol{c}^k F_{\boldsymbol{\lambda}}(\boldsymbol{x}-\boldsymbol{x}^k) \quad \forall k \in [\![1,N]\!], \tag{7}$$

where $F_{\boldsymbol{\lambda}}$ is a shape function, discussed in Sub-Section III-C. As for the intensity $\boldsymbol{c}^k$, its three components are defined as:

$$c_i^k = \sum_{j=1}^{3} a_{i,j}\epsilon_{i,j}^k \quad \forall i \in \{1,2,3\}, \quad \forall k \in [\![1,N]\!]. \tag{8}$$

All instances of $\epsilon_{i,j}^k$ are independent random values that follow a normal or Gaussian distribution centered around 0 with a variance of 1, representing the random aspect of turbulence. The terms $a_{i,j}$ are the elements of a matrix A, which is the Cholesky decomposition of the Reynolds Stress Tensor $\overline{\overline{\boldsymbol{R}}}$:

$$\overline{\overline{\boldsymbol{R}}} = \begin{pmatrix} R_{1,1} & R_{1,2} & R_{1,3} \\ R_{2,1} & R_{2,2} & R_{2,3} \\ R_{3,1} & R_{3,2} & R_{3,3} \end{pmatrix} = \overline{\overline{\boldsymbol{A}}}\,\overline{\overline{\boldsymbol{A}}}^{T} \quad \text{with} \quad \overline{\overline{\boldsymbol{A}}} = \left(a_{i,j}\right) \tag{9}$$

Through Equations (8) and (9), the link between the intensities $\boldsymbol{c}^k$ of the turbulent structures and the Reynolds Stress Tensor $\overline{\overline{\boldsymbol{R}}}$ ensures the generation of a velocity field that statistically replicates any given turbulence intensity I_∞ and any given anisotropic ratio (σ_u:σ_v:σ_w) [2], [9]. Indeed the three components of the anisotropic ratio (σ_u:σ_v:σ_w) are given by the square roots of the diagonal components of the Reynolds Stress Tensor $\overline{\overline{\boldsymbol{R}}}$. Thus the turbulent intensity I_∞ can be rewritten as a function of the trace of the Reynolds Stress Tensor $\overline{\overline{\boldsymbol{R}}}$:

$$I_\infty = \frac{100}{|\boldsymbol{u}^{\infty}|}\sqrt{\frac{\mathbf{tr}\left(\overline{\overline{\boldsymbol{R}}}\right)}{3}} \tag{10}$$

This last Equation (10) ensures that the turbulent field will have the desired turbulent intensity I_∞ and anisotropic ratio (σ_u:σ_v:σ_w).

C. Definition of the shape function and the structure sizes

The next step in the definition of the reformulated Synthetic Eddy Method is the characterisation of the shape function $F_{\boldsymbol{\lambda}}$, appearing in Equation (7). It is expressed as prescribed by Jarrin *et al.*:

$$F_{\boldsymbol{\lambda}}(\boldsymbol{y}) = \prod_{i=1}^{3} f_{\lambda_i}(y_i). \tag{11}$$

$\boldsymbol{\lambda}$ determines the size of the area of influence of each turbulent structure k. This size could be naively interpreted as one of the well-known turbulent length scales (such as Taylor or Kolmogorov length scales), but its implementation is not as straightforward. These aspects will be investigated in Sections IV and V.

The fact that $\boldsymbol{\lambda}$ is defined as a vector of the area of influence to have different sizes λ_i in each direction i. Each individual turbulent structure k could also have its own vector size $\boldsymbol{\lambda}_k$, as will be discussed in the following Sections.

For the first preliminary results presented in Section IV, a basic shape function $F_{\boldsymbol{\lambda}}$ given by Jarrin *et al.* is used.

This basic tent function belongs to the C^0-class functions: it is continuous but its first derivative presents large discontinuities. In the framework of Lagrangian Vortex computations, such discontinuities in the velocity derivatives can be problematic, more specifically for the evaluation of the stretching term $\mathcal{S}_i V_i$ as presented in Equation (2). Smoother alternative shape functions f_λ can be defined, such as a Gaussian function used in the remainder of this study:

$$f_\lambda(y) = \begin{cases} c(\lambda) \left(1 - \frac{e^1\, y^2}{\lambda^2} \exp(-\frac{y^2}{\lambda^2})\right) & \text{if } -\lambda \leq y \leq \lambda \\ 0 & \text{otherwise} \end{cases} \tag{12}$$

where $c\,(\lambda) = \frac{1}{\sqrt{L\ (\frac{25}{8} + \frac{3\ e^2\ \sqrt{\pi} * \mathrm{erf}(\sqrt{2})}{16\sqrt{2}} - e^1\ \sqrt{\pi} * \mathrm{erf}(1)\ )}}$.

D. Enabling variation in the turbulence structure sizes

The theory of turbulent scales dictates that every turbulent flow contains a wide range of whirlpools of various magnitudes. Despite its purely mathematical nature, the purpose of this model remains to best represent the true physical phenomenon of turbulent agitation. Thus a standard deviation of the size of turbulent structures, denoted $\sigma(\lambda)$, is added as a parameter of the model. At deviation zero, all turbulent structures k will have the same size $\boldsymbol{\lambda}$. A non-zero value of deviation will result in a term $\sigma(\lambda)$ being added into the size of each turbulent structure, generating turbulent structures ranging in size. The added term $\sigma(\lambda)$ is computed so as to assure that these sizes are normally distributed: $\lambda \sim \mathcal{N}\ (\lambda,\ \sigma^2(\lambda)\ )$ in each independent dimension $i = 1, 2, 3$. The standard deviation $\sigma(\lambda)$ is expressed as a percentage of the variable λ, for instance: $\sigma(\lambda) = 10\% = 0.1\ \lambda$. In all cases, this will result in a more or less wide spread of turbulent structure sizes, centered around the average given by the prescribed values of $\boldsymbol{\lambda}$.

E. Integration of the Synthetic-Eddy-Method into the Vortex method

The Vortex Particle Method presented in Section II is an unsteady Lagrangian method in an unbounded domain, where the fluid domain is considered to be infinite. However, as mentioned in Sub-Section III-B, the Synthetic Eddy Method requires the definition of a set volume $\tilde{V}$ containing all the turbulent structures. To this end a study space E_S of volume $\tilde{V}$ is defined, inside which the artificial ambient turbulence is desired (see Fig. 1).

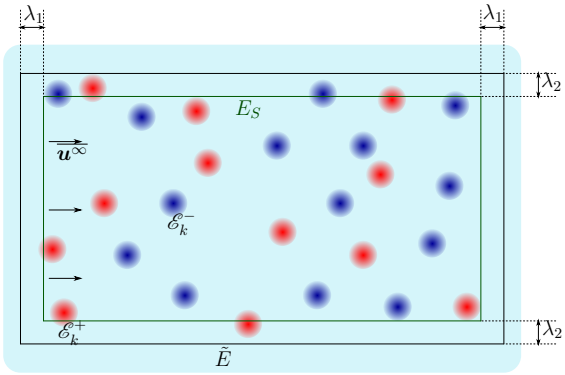

Fig. 1. Schematic view of the integration of the Synthetic-Eddy-Method into the Vortex method

The turbulent structures are generated by the Synthetic Eddy Method inside a second larger space $\tilde{E}$, designed so that one turbulent structure can fit in between the two nested spaces, to ensure the uniformity of the fluctuations all over the actual area of interest. N turbulent structures k are generated within the chosen space $\tilde{E}$, at random initial positions and of sizes distributed around the average vector size $\boldsymbol{\lambda}$, as discussed in the previous Sub-Section. After their initialization, the turbulent structures are advected with the flow as the simulation progresses. If during the course of the simulation a turbulent structure is advected outside of the boundaries of the sapce $\tilde{E}$, it is deleted, and replaced by a newly generated structure at the inlet of the space.

Each newly generated turbulent structure k is assigned an intensity $\boldsymbol{c}^k$, calculated using Equation (8), and a random variable $\epsilon_{i,j}^k$, which has equal probabilities of being equal to 1 or -1.

In this preliminary study, the simplest level of coupling is selected: advecting the turbulent structures with the constant velocity $\overline{\boldsymbol{u}^\infty}$, and omitting their influence in the calculation of stretching and diffusive terms of the Navier-Stokes equation. Thus in our application, further detailed in Section VI, the turbulent structures function as an under-layer: they influence the velocity distribution on the turbines and in their wake, without being influenced reciprocally.

As an alternative to setting an arbitrary number of turbulent structures N, their saturation level within the study space is characterized by the filling ratio R_f:

$$R_f = \sum_{k=1}^{N} \frac{V_k}{\tilde{V}} \tag{13}$$

where V_k is the volume of the area of influence of the structure k (for instance if $\lambda_1 = \lambda_2 = \lambda_3$, $V_k = \frac{4}{3}\pi\lambda_1^3$).

IV. Numerical reconstruction of the ambient turbulent velocity field

In order to better study the turbulent flows generated by the Synthetic Eddy Method and the influence of the various turbulent parameters, numerically generated flows are first studied in the absence of turbines.

F. Reconstructed velocity field

Fig. 2 (a)-(b) shows examples of turbulent flow fields generated with the Synthetic Eddy Method for different values of turbulent intensity I_∞. At first glance, these flows appear to be very realistic, with the disruptions to the flow field increasing with the value of the turbulent intensity.

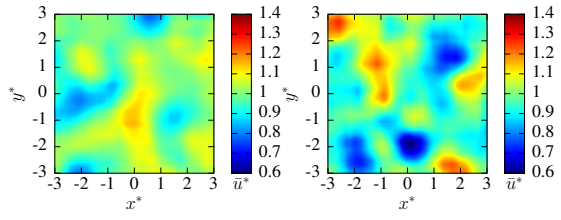

(a) $I_\infty = 5\%$ (b) $I_\infty = 10\%$

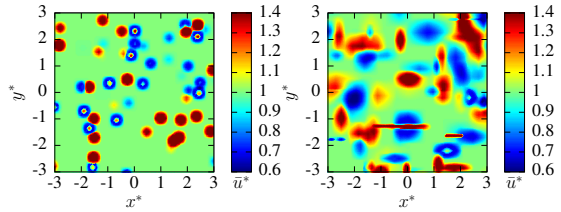

(c) $\boldsymbol{\lambda} = (0.25, 0.25, 0.25)$ (d) $\sigma(\lambda) = 50\%$, $\boldsymbol{\lambda} = (0.5, 0.5, 0.5)$

Fig. 2. Examples of velocity fields provided by the Syntehtic Eddy model for $N = 1000$ structures and different sets of parameters. The dimensions of the displayed plane are 6x6. Unless captioned otherwise, the parameters used are the following: $I_\infty = 15\%$, $\boldsymbol{\lambda} = (1, 1, 1)$, $\sigma(\lambda) = 0\%$.

The size of the turbulent structures, set to $\boldsymbol{\lambda} = (1, 1, 1)$, is not immediately apparent. Fig. 2 (c) shows the influence of this size parameter. When the turbulent structures are small, each structure can be clearly identified; whereas when the size increases, individual structure shapes are lost in the overlap.

Fig. 2 (d) shows the influence of the variation $\sigma(\lambda)$ allowed on the turbulent structure sizes $\boldsymbol{\lambda}$. For higher variations $\sigma(\lambda)$, the shape of the turbulent structures becomes increasingly eclectic and diverse.

G. Numerical reconstruction of the Reynolds Stress Tensor

The main function of the Synthetic Eddy Method is its ability to reproduce any given Reynolds Stress Tensor. Before integrating this method into turbine simulations, the accuracy of this reproduction must be verified. This will ensure the correct representation of any given turbulence intensity I_∞ and anisotropic ratio (σ_u:σ_v:σ_w), as their direct link to the Reynolds Stress Tensor is made clear in Equation (10).

In order to simplify this verification, one unique quantity is examined: the Turbulent Kinetic Energy (TKE) K as defined in the following Equation.

$$K = \frac{1}{2}(\sigma_u^2 + \sigma_v^2 + \sigma_w^2) \tag{14}$$

The value of K is calculated based on the velocity time series recorded at a single point in a turbulent flow, as it would be in the context of an experimental study. To this end, a turbulent space $\tilde{E}$ is built around the sampling point. Turbulent structures evolve within this space, advected with a prescribed upstream velocity of $\boldsymbol{U}^\infty = (1, 0, 0)$ m/s. Various parameters are tested, such as the size of turbulent structures $\boldsymbol{\lambda}$, the variation on the size of the turbulent structures $\sigma(\lambda)$, and the filling ratio R_f as defined in Equation (13).

Each time series is generated over a simulated period of 12 hours, with a sampling interval of $dt = 0.1$ seconds. However due to the probabilistic nature of the Synthetic Eddy Method, the results are not strictly reproducible for any given set of parameters. In order to obtain an accurate representation of the value of K to be expected, 50 time series are computed for each set of parameters. The average and maximal error on the value of K out of the 50 trials are measured for each set of parameters.

With the physical turbulence parameters of $I_\infty = 3\%$ and the prescribed Reynolds tensor mentioned above, the expected theoretical value of the TKE is set at 1.35×10^{-3}.

Fig. 3 shows the average and maximal errors on the reconstructed TKE for different values of the turbulent structure sizes $\boldsymbol{\lambda}$ and filling ratio R_f. For all structure sizes $\boldsymbol{\lambda}$, the average error on the TKE is at its lowest lowest for the higher filling ratios R_f. Additionally, the relative position of each average error curve shows that the error on the TKE is lower for smaller structure sizes $\boldsymbol{\lambda}$.

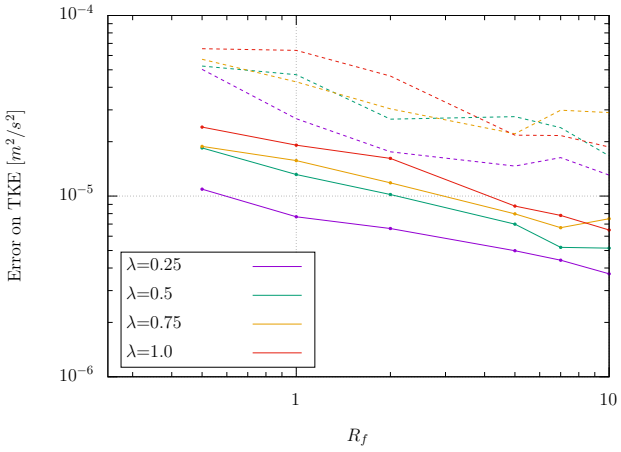

Fig. 3. Average error (full lines) and maximal error (dashed lines) on the value of the TKE K plotted against the filling ratio R_f, for various size of turbulent structures $\boldsymbol{\lambda}$. In all cases: $I_\infty = 3\%$, $\sigma(\lambda) = 0\%$, and the sub-function f_λ uses the Gaussian kernel.

Fig. 4 shows the same average and maximal errors on the TKE for different structure sizes $\boldsymbol{\lambda}$, plotted now over a variance $\sigma(\lambda)$ allowed around the average sizes $\boldsymbol{\lambda}$. This graph shows a slight increase in the value of the errors for higher variances $\sigma(\lambda)$. The difference between the curves corresponding to different average sizes $\boldsymbol{\lambda}$ is no longer evident. The blurring of these differences could be explained by the introduction of size variation $\sigma(\lambda)$, meaning that turbulent structures are no longer all of the exact same size $\boldsymbol{\lambda}$ for each curve.

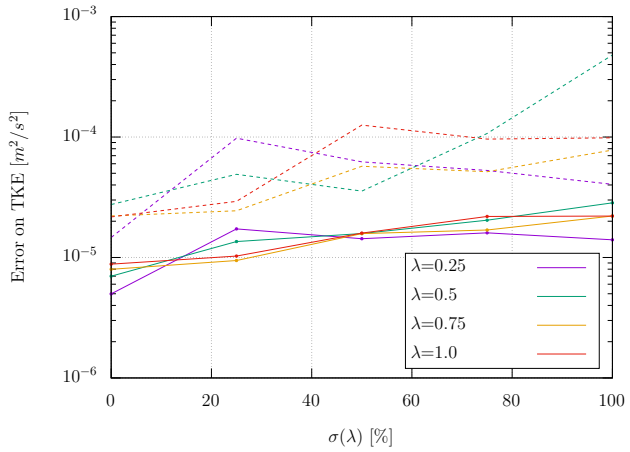

Fig. 4. Average error (full lines) and maximal error (dashed lines) on the value of the TKE K plotted against the variance $\sigma(\lambda)$ allowed around average turbulent structure sizes $\boldsymbol{\lambda}$, for various size of turbulent structures $\boldsymbol{\lambda}$. In all cases: $I_\infty = 3\%$, $R_f = 5$, and the sub-function f_λ uses the Gaussian kernel.

These tests show that for all sets of parameters, the error committed on the value of the TKE, ranging around 10^{-5}, is always satisfyingly low compared to the expected value of 1.35×10^{-3}. However it can be concluded that the Reynolds Stress Tensor is more accurately reproduced when using a high number of turbulent structures of small size $\boldsymbol{\lambda}$. Introducing variation on the sizes of the turbulent structures also slightly disrupts its components.

V. Physical analysis of the reconstructed turbulent flow

In order to pursue the analysis of numerical flows generated by the Synthetic Eddy Method, velocity spectra can also be considered, as is done by Medina [10]. Two characteristic physical behaviors of the turbulent flow are analyzed. Firstly the time-averaged instantaneous power spectral density (PSD) of the velocity field in the Fourier space illustrates the principle of energy decay in a turbulent flow. Secondly the integral length scale of the flow, also called Taylor macroscale, gives a representation of the size of the generated turbulent structures.

H. Spectral analysis

The synthetic turbulence generation method is based on a stochastic algorithm. The statistical properties of turbulent kinetic energy can be described by energy distribution spectra, commonly represented in a logarithmic scale over the wavenumber of the turbulent structures.

The purpose of this study is not to measure the kinetic energy along the wavenumber, but rather to paint a picture of the global behaviour of the kinetic energy in the numerically generated turbulent flow. We focus here on the velocity fluctuations at a single central point in the flow, caused by the presence of N generated turbulent structures.

Velocity time series recorded at this point are now used to calculate spectra, based on the variations in the driving axis of the flow. Fig. 5 shows the power spectral density for a fixed average size $\boldsymbol{\lambda}$ of turbulent structures and various values of the size variation $\sigma(\lambda)$.

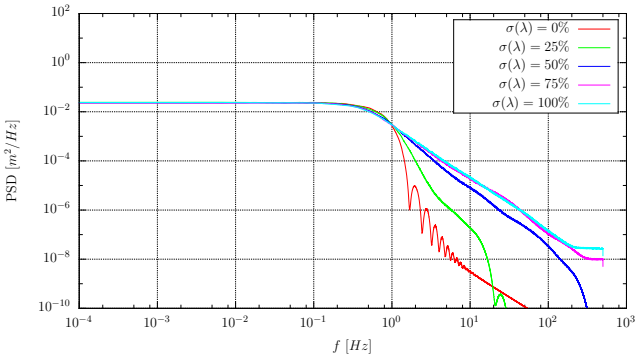

Fig. 5. Influence of $\sigma(\lambda)$ on the spectral representation for a Gaussian kernel, with $\boldsymbol{\lambda} = (0.5, 0.5, 0.5)$ and $R_f = 2$.

While all PSD curves show the evidence of a general energy decay, this decay is not always linear, but disrupted by recurring "bumps" in the absence of strucure size variation $\sigma(\lambda)$. These "bumps" are explained by the nature of the Fourrier transform used to compute the PSD, when applied to a sum of kernel functions of identical width λ.

However when the standard deviation $\sigma(\lambda)$ on the size of turbulent structures is nonzero, the flow is filled with a range of structures of different sizes. The Fourrier transform of the velocity signal becomes a sum of now staggered "bumpy" elements, leading to a smoother end result. This PSD curve appears to converge with respect to the variation $\sigma(\lambda)$ as of $\sigma(\lambda) = 75\%$, towards a quasi-linear energy decay.

Similar results are obtained with both types of sub-function kernels f_λ. This shows the importance of introducing a wide enough range of structure sizes, in order to accurately reproduce the behavior expected of a realistic turbulent flow.

I. Comparison with experimental data

With sufficient variation on the size of the turbulent structures, the PSD now displays a realistic behavior. However it has yet to be validated by comparison with experimental spectra calculated from real turbulent flows. The work of Medina *et al.* [11] provides such data, for an upstream velocity of $\boldsymbol{u}_\infty = 0.8$ m/s and a turbulent intensity of $I_\infty = 15\%$. Fig. 6 compares this experimental data with the numerically obtained results, for different average sizes of turbulent structures, and a variation in these sizes of $\sigma(\lambda) = 100\%$. In all cases, the correspondence between numerical and experimental data appears to be very satisfying. This result validates the generation of turbulent flows by the Synthetic Eddy Method: it can be concluded that the synthetic turbulence reproduces the accurate energy behavior of a real turbulent flow.

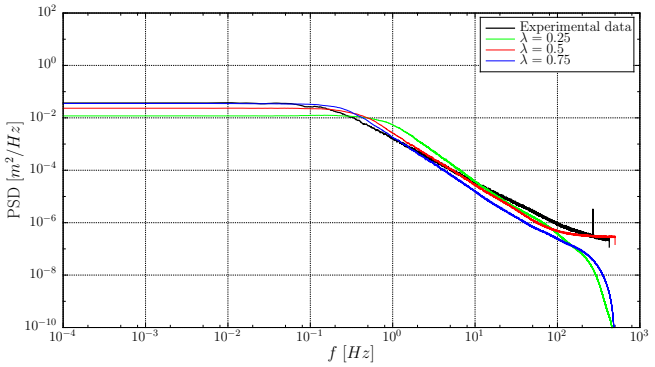

Fig. 6. Comparison between numerical and experimental data, with the Gaussian kernel sub-function, $\sigma(\lambda) = 100\%$, $I_\infty = 15\%$, and $\boldsymbol{U}_\infty = 0.8$ m/s.

J. Autocorrelation and the Taylor scale $\mathcal{L}$

True physical turbulent motions occur over a wide range of time and length scales, with the largest scales accounting for the largest transports of momentum and energy. In this case, we attempt to link the spatial scale of the turbulent behavior in the numerically generated flow to the prescribed sizes λ of the turbulent structures. There are many possible methods to measure the scales of turbulent behavior in a given flow. One such measure is the Taylor macroscale $\mathcal{L}$, which gives an estimate of the characteristic size of turbulent eddies. $\mathcal{L}$ is calculated using the autocorrelation method based once again on the fluid velocity measured at a single point over a period of time:

$$\mathcal{L} = \overline{u} \int_0^\infty R(\tau)\mathrm{d}\tau \tag{15}$$

with $R(\tau)$, the autocorrelation fonction.

The characteristic length $\mathcal{L}$ of the flow is calculated for varying turbulent structure sizes $\boldsymbol{\lambda}$, with no variance $\sigma(\lambda)$ allowed. The results displayed in Fig. 7 shows a near-linear relationship obtained between the prescribed size λ and the resulting turbulent spacial scale $\mathcal{L}$, evidenced using a linear regression model. This study yields similar results for the triangular kernel sub-function f_λ.

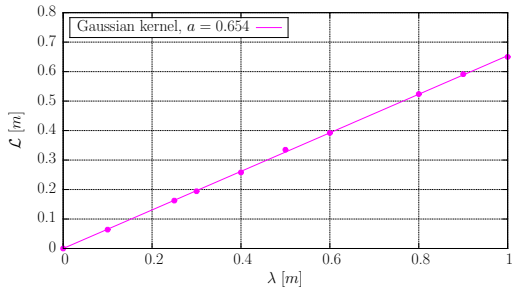

Fig. 7. Linear relation between $\mathcal{L}$ et λ (Gaussian kernel).

The turbulent scale $\mathcal{L}$ is now recalculated with the introduction of variances $\sigma(\lambda)$ around the average structure sizes λ. Table I shows that this results in only small disruptions of the value of the scale $\mathcal{L}$. It can thus be assumed that with or without variation on the size λ of the turbulent structures, λ is proportional to the scale of the turbulent behavior in the generated flow.

TABLE I
INFLUENCE OF THE VARIATION ON THE STRUCTURE SIZES $\sigma(\lambda)$ ON THE VALUE OF THE TAYLOR MACROSCALE $\mathcal{L}$ WITH $R_f = 1$ AND THE GAUSSIAN KERNEL.

$\sigma(\lambda)$ (%)	0	25	50	75	100
$\mathcal{L}$ $(\lambda = 0.25)$	0.163	0.163	0.162	0.162	0.169
$\mathcal{L}$ $(\lambda = 0.5)$	0.330	0.336	0.310	0.327	0.328
$\mathcal{L}$ $(\lambda = 0.75)$	0.496	0.478	0.474	0.486	0.518

VI. Numerical results with marine current turbine

The properties of the turbulent flows generated by the SEM have been thoroughly studied in the absence of turbines. It can now be verified how well these flows fulfil their purpose of showing the influence of ambient turbulence in the surrounding flow on the behavior of a tidal turbine.

K. Simulation conditions

Single turbine simulations are performed with turbulent intensities ranging from 0 to 15%, which is the highest turbulent intensity reproducible in the IFREMER flume tank for later comparison with experimental data.

These simulations are initially carried out with a simplified turbine model: only the three turbine blades are represented. The turbine hub is omitted in order to avoid any possible numerical instabilities that can occur when turbulent structures push fluid particles sideways into its mesh.

90 seconds of physical time are simulated, and velocity averages are post-treated over the last 50 seconds once the turbine wake is stabilised. The velocity component $\tilde{u}$ produced by the SEM, as mentioned in Equation (5), is omitted from this post-treatment, in order to emulate the effect of a longer time average.

For these first simulations, small turbulent structures of size $\boldsymbol{\lambda} = (0.5, 0.5, 0.5)$ are used with no variation $\sigma(\lambda)$ on these sizes allowed. Turbulent structures are set to cover the entirety of the study space, with the filling ration $R_f = 1$.

L. Influence of the turbulent intensity

Fig. 8 shows the velocity maps of turbine wakes obtained in these conditions for varying turbulent intensities I_∞. Despite the evidence of the missing hub in the form of a heightened velocity at the center of the wake, satisfying tendencies can be observed.

First of all, in the absence of ambient turbulence, the turbine wake extends to approximately 10 diameters behind the rotor, which is the correct behavior expected in low turbulence conditions [12]. Secondly, when using and progressively increasing the ambient turbulence intensity generated by the SEM, the turbine wake becomes progressively shorter. This is further evidenced when considering the velocity deficits integrated in the wake of the turbine. By the relative positioning of the velocity deficit curves, Fig. 9 confirms the ever faster wake recovery as the turbulent intensity is increased.

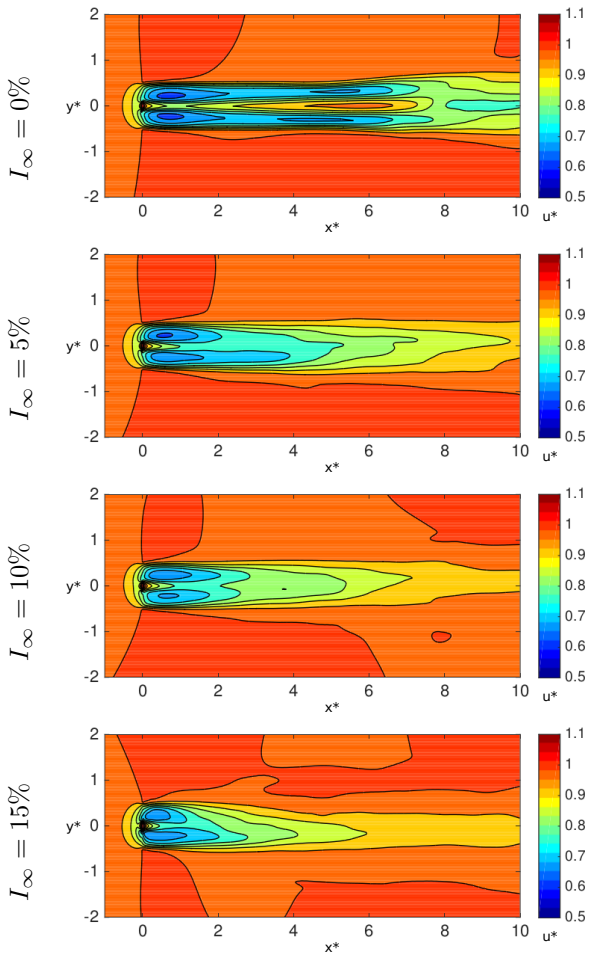

Fig. 8. Velocity maps in the wake of a single turbine, averaged over a period of 50 seconds, for varying levels of turbulent intensity.

The Synthetic Eddy Method thus proves its compatibility with the full marine turbine Vortex simulation software. In addition to its ability to reproduce physical properties of experimental flows, it can also have the correct influence on the wake of the turbine, in the form of the shortening of its wake, also observed in experimental studies conducted at IFREMER [1].

VII. Conclusions and Further works

The important role played by the ambient turbulence intensity on marine current turbines' behavior is addressed by the means of numerical simulation. In the simulation code developed at LOMC in collaboration with IFREMER, a new module based on the Synthetic Eddy Method initially proposed by Jarrin *et al.* [2] [3] represents ambient turbulence around marine current turbines.

This ambient turbulence model is able to generate a perturbed flow verifying any given turbulence intensity I_∞ and any anisotropic ratio (σ_u:σ_v:σ_w). With the correct parameters, the Power Spectral Density is satisfyingly aligned with experimental results, and a remarkable relation is evidenced between the size of turbulent structures and turbulent behavior in the flow. Its compatibility with the turbine simulation software

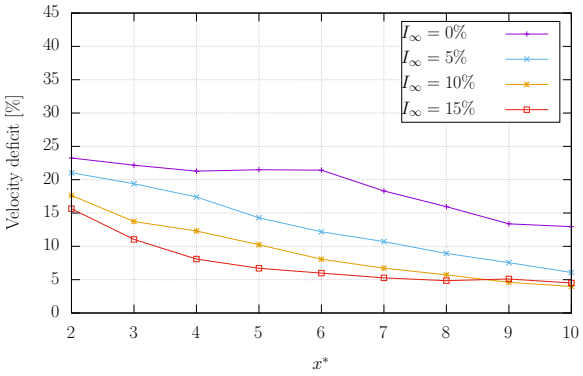

Fig. 9. Velocity deficit integrated at set distances in the wake of a single turbine, for varying levels of turbulent intensity I_∞. The velocity deficit is calculated as a percentage representing the velocity deficit compared to the average upstream velocity U_∞, when integrated on a disc of the same width as the turbine and at given distances behind its center.

is proven by the quality of the first wake simulation results.

A more detailed study is in progress of the influence of the various parameters of the SEM on the simulated turbine wakes. Once this has been accomplished, simulations can be carried out using more than one turbine, the end goal of this study being the simulation of an entire marine turbine farm in various turbulent conditions.

As a development to the SEM itself, the fact that the present implementation is not divergence-free must be addressed. For the turbulent intensities considered here the error in the flow poses no considerable issue. Further work is needed in order to reformulate the velocity perturbation term $\tilde{\boldsymbol{u}}$, in a way that is compatible with the present Vortex formulation.

References

[1] P. Mycek, B. Gaurier, G. Germain, G. Pinon, and E. Rivoalen, "Experimental study of the turbulence intensity effects on marine current turbines behaviour. part I: One single turbine," *Renewable Energy*, vol. 66, no. 0, pp. 729 – 746, 2014. [Online]. Available: http://www.sciencedirect.com/science/article/pii/S096014811400007X

[2] N. Jarrin, S. Benhamadouche, D. Laurence, and R. Prosser, "A synthetic-eddy-method for generating inflow conditions for large-eddy simulations," *International Journal of Heat and Fluid Flow*, vol. 27, pp. 585–593, 2006.

[3] N. Jarrin, "Synthetic inflow boundary conditions for the numerical simulation of turbulence," Ph.D. dissertation, University of Manchester, 2008.

[4] C. Rehbach, "Calcul numrique d'coulements tridimensionnels instationnaires avec nappes tourbillonaires," *La Recherche Arospatiale*, vol. 5, pp. 289–298, 1977.

[5] R. Lewis, *Vortex element methods for fluid dynamic analysis of engineering systems*. Cambridge University Press, 1991.

[6] G. Cottet and P. Koumoutsakos, *Vortex methods: theory and practice*. Cambridge University Press, 2000.

[7] G. Pinon, P. Mycek, G. Germain, and E. Rivoalen, "Numerical simulation of the wake of marine current turbines with a particle method," *Renewable Energy*, vol. 46, no. 0, pp. 111 – 126, 2012. [Online]. Available: http://www.sciencedirect.com/science/article/pii/S0960148112002418

[8] G. Pinon, C. Carlier, A. Fur, B. Gaurier, G. Germain, and E. Rivoalen, "Account of ambient turbulence for turbine wakes using a synthetic-eddy-method," *Journal of Physics: Conference Series*, vol. 854, no. 1, pp. 012–016, 2017. [Online]. Available: http://stacks.iop.org/1742-6596/854/i=1/a=012016

[9] T. S. Lund, X. Wu, and K. D. Squires, "Generation of turbulent inflow data for spatially-developing boundary layer simulations," *Journal of Computational Physics*, vol. 140, pp. 233–258, 1998.
[10] O. D. Medina, F. Schmitt, R. Calif, G. Germain, and B. Gaurier, "Correlation between synchronised power and flow measurements, a way to characterize turblence effecs on marine current turbine." in *11th European Wave and Tidal Energy Conference (EWTEC)*, September 2015, Nantes, France.
[11] O. D. Medina, F. Schmitt, R. Calif, G. Germain, and B. Gaurier, "Caractérisation expérimentale du sillage généré par une hydrolienne - influence du taux de turbulence ambiant," in *14mes Journes de l'Hydrodynamique*, Novembre 2014, val de Reuil, France.
[12] C. Carlier, G. Pinon, B. Gaurier, G. Germain, and E. Rivoalen, "A synthetic eddy-method to represent the ambient turbulence in numerical simulation of marine current turbine," in *10th European Wave and Tidal Energy Conference (EWTEC)*, September 2015, Nantes, France.